The hepatitis C virus 3′-untranslated region or a poly(A) tract promote efficient translation subsequent to the initiation phase

Shelton S. Bradrick, Robert W. Walters and Matthias Gromeier*

Department of Molecular Genetics and Microbiology, Duke University Medical Center, Durham, NC 27710, USA

ABSTRACT

Enhancement of eukaryotic messenger RNA (mRNA) translation initiation by the 3′ poly(A) tail is mediated through interaction of poly(A)-binding protein with eukaryotic initiation factor (eIF) 4G, bridging the 5′ terminal cap structure. In contrast to cellular mRNA, translation of the uncapped, non-polyadenylated hepatitis C virus (HCV) genome occurs independently of eIF4G and a role for 3′-untranslated sequences in modifying HCV gene expression is controversial. Utilizing cell-based and *in vitro* translation assays, we show that the HCV 3′-untranslated region (UTR) or a 3′ poly(A) tract of sufficient length interchangeably stimulate translation dependent upon the HCV internal ribosomal entry site (IRES). However, in contrast to cap-dependent translation, the rate of initiation at the HCV IRES was unaffected by 3′-untranslated sequences. Analysis of post-initiation events revealed that the 3′ poly(A) tract and HCV 3′-UTR improve translation efficiency by enabling termination and possibly ribosome recycling for successive rounds of translation.

INTRODUCTION

Translation of cellular messenger RNA (mRNA) depends upon a 5′ m^{7}GTP cap structure that mediates recruitment of eukaryotic initiation factor (eIF) 4F, a multi-protein complex required for association of the 43S pre-initiation complex [reviewed in (1)]. Notably, canonical mRNA translation also critically depends on the presence of poly(A)-binding protein (PABP) bound to the 3′ poly(A) tail [reviewed in (2)]. PABP enhances initiation through binding the eIF4G component of eIF4F (3), conceivably promoting circularization of the mRNA template. Interaction of PABP with eIF4G increases the affinity of eIF4E for the cap structure (4).

Moreover, PABP has been suggested to improve formation of 80S ribosomal intermediates through a role in 60S subunit joining (4,5). Besides the poly(A) tail, a modulatory role for 3′-untranslated elements in translation has also been reported for non-polyadenylated viral and cellular templates, including histone, rotavirus and dengue virus mRNAs (6–8). Thus, although the structure of terminal features among coding RNAs differ dramatically, putative 5′–3′ interactions may play a crucial role in the control of translation rate in general.

Hepatitis C virus (HCV) is a significant blood-borne pathogen responsible for liver failure, cirrhosis and hepatocellular carcinoma in chronically infected patients [reviewed in (9)]. As a positive-strand RNA virus of *Flaviviridae*, HCV genomic RNA directly serves as template for the production of a large polyprotein that is processed into at least 10 structural and non-structural gene products. To facilitate expression of viral proteins at the uncapped viral genome, HCV utilizes a highly structured internal ribosomal entry site [IRES; (10)] located within the 5′-untranslated region (UTR). Remarkably, the HCV IRES directly binds the 40S ribosomal subunit (11), forming a binary complex in the absence of eIFs. Subsequent recruitment of eIF3 and ternary complex (Met-tRNA•eIF2α•GTP) leads to formation of a 48S* intermediate in which the start codon is properly positioned in the ribosomal P-site (12,13). Hydrolysis of GTP with concomitant release of initiation factors allows 60S subunit joining and formation of an 80S ribosomal complex that is competent for the elongation phase of translation.

The ~220 nt 3′-UTR of HCV is non-polyadenylated and composed of three distinct regions (Figure 1B): a poorly conserved segment immediately downstream of the stop codon termed the variable region, a poly(U/UC) tract of heterogenous length and the highly structured 98 nt X-region (14). Crucial *cis*-acting signals for viral RNA synthesis are located within the HCV 3′-UTR and, while clearly essential for viral replication (15), a potential role for the HCV 3′-UTR in viral translation is contentious. Indeed, HCV 3′-UTR sequences have been variously reported to either

*To whom correspondence should be addressed. Tel: +1 919 668 6205; Fax: +1 919 684 8735; Email: grome001@mc.duke.edu
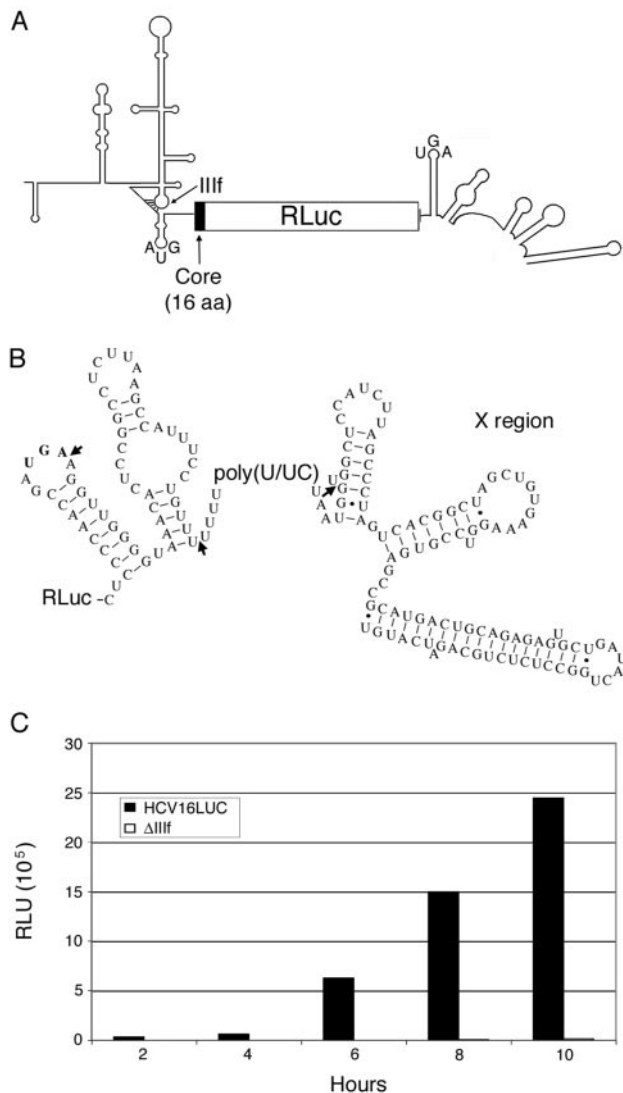
Figure 1. Efficient translation of subgenomic HCV reporter RNA depends upon higher order RNA structure. (**A**) Schematic representation of HCV16LUC reporter RNA. The positions of IRES domain IIIf and conserved pseudoknot are indicated. (**B**) Sequence and secondary structure of the HCV 3′-UTR. Arrows indicate locations of 3′ terminal deletions assayed for translation efficiency in Huh7 cells (Figure 2). The authentic stop codon is indicated in bold letters. (**C**) Huh7 cells were transfected with 0.2 μg of indicated reporter RNAs and RLuc was measured by enzymatic assay over the course of 10 h after the start of transfection.

stimulate activity of the IRES (16–19), have no effect at all (20–23), or even down-regulate translation (24). Additionally, mechanistic details have failed to emerge for either proposed positive or negative effects of the HCV 3′-UTR on IRES-dependent translation.

In an effort to clarify the role of 3′-UTR sequences in HCV translation control, we uncovered an unexpected role for the poly(A) tail in translation control. Employing a combination of cell-based and *in vitro* translation assays, we report that either the native HCV 3′-UTR or a poly(A) tract of sufficient length significantly enhance IRES-dependent translation. Investigating the underlying mechanism for these observations, we find that stimulatory 3′ sequences do not regulate the accumulation

of initiation intermediates, but rather act at a step downstream of initiation. The results presented here suggest that native HCV 3′-untranslated sequences or a poly(A) tract of sufficient length regulate translation by increasing the efficiency of termination and, possibly, ribosome recycling.

MATERIALS AND METHODS

Cell cultures

Huh7 human hepatoma cells (obtained from E. Wimmer, SUNY-Stony Brook) were maintained in DMEM containing 10% fetal bovine serum, non-essential amino acids, 200 μM L-glutamine, 10 U/ml penicillin, 10 μg/ml streptomycin and 0.25 μg/ml amphotericin B. HeLa S3 spinner cells were obtained from the Duke Cell Culture Facility and propagated as previously described (25).

Plasmid constructions

A plasmid clone of the complete HCV 1a genome [H77 strain; obtained from E. Schmidt, Harvard University] was utilized for generation of all HCV reporter constructs. HCV16LUC was constructed by the following method: the HCV IRES, including 16 codons of the core gene, and an upstream portion of the gene for *Renilla* luciferase (RLuc) were PCR amplified using standard conditions. The resulting DNA fragments were subsequently 'fused' (26) in a second PCR and digested with AgeI and XmnI. For assembly of the 3′ region of HCV16LUC, a downstream RLuc region and five codons of NS5B plus the HCV 3′-UTR were individually amplified, fused and digested with XmnI and AflII. HCV16LUC was subsequently cloned by ligation of the upstream and downstream fragments into vector prepared from the H77 full-length plasmid using AgeI and AflII. All plasmid clones described were verified by sequencing.

Reporter construct containing the CBV3 3′-UTR (HCV-CBV3) was generated by insertion of the NotI–XmnI fragment from HCV16LUC into vector prepared from a CBV3 RLuc reporter plasmid (27). Vector sequences for non-specific 3′-UTRs were obtained from pGEM-9Zf(−) bases 76–375 (Promega) by PCR amplification. Generation of polyadenylated variants of HCV16LUC was performed as follows: complementary oligonucleotides containing poly(A_{12} or A_{50}) with XbaI and ClaI overhangs were annealed and inserted into vector prepared from the HCV-CBV3 reporter construct to yield polyadenylated reporters lacking HCV 3′-UTR sequences. A PCR-amplified HCV 3′-UTR fragment was cloned into polyadenylated constructs digested with XbaI and blunt ended with Klenow DNA polymerase to generate polyadenylated constructs containing the 3′-UTR. To generate the β-globin leader containing construct for capped mRNAs, the *RLuc* gene was inserted into pTnT vector (Promega) using XbaI and XhoI.

Template preparation and *in vitro* transcription

In order to produce reporter RNAs with authentic 5′ and 3′ ends, standard PCR using *Vent* DNA polymerase (New England Biolabs) was performed to generate template DNA for *in vitro* transcription. Transcripts were designed to initiate with G(+1)C(+2) corresponding to the authentic 5′ terminus of the HCV genome. Transcription templates were subjected to

1.5% agarose gel electrophoresis and purified by gel extraction (Qiagen). Templates for polyadenylated HCV reporter constructs were prepared by digestion of plasmid with ClaI. For capped β-globin transcription, plasmid was linearized with BamHI or NotI to produce template for containing or lacking a 30 residue poly(A) tail, respectively.

   In vitro transcription reactions were performed with 1 μg template using T7 RNA polymerase (New England Biolabs) according to the manufacture's protocol and then treated with 5 U DNase I (Ambion). RNAs were then purified using the RNeasy kit (Qiagen) and quantified by UV spectrophotometry. RNA transcripts were examined for quality by agarose gel electrophoresis followed by visualization with ethidium bromide.

RNA transfection and luciferase assays

For analysis of reporter RNA translation rates *in vivo*, Huh7 cells (400 000 cells per 3.5 cm plate) were co-transfected with 0.2 μg HCV RLuc RNA and capped FLuc RNA using DMRIE-C reagent (Invitrogen). At 2 h post-transfection, the transfection mixture was aspirated from cells and replaced with supplemented DMEM lacking antibiotics. At indicated time points after the start of transfection, cells were washed with phosphate-buffered saline and scraped in 0.2 ml lysis buffer (Promega). Luciferase levels were determined in 20 μl aliquots of lysed cells using the dual luciferase assay system (Promega) and a Berthold luminometer (LB 9507).

Assay for RNA stability *in vivo*

To examine decay rates of reporter RNAs *in vivo*, cells were transfected as described above with [α-^{32}P]UTP labeled RNA. At each time point cells were washed twice with phosphate-buffered saline, scraped in lysis buffer (400 mM $KOAc_2$, 25 mM HEPES-KOH pH 7.4, 15 mM $MgCl_2$ and 2% digitonin) and incubated 30 min on ice. Cell debris was removed by centrifugation and soluble RNA was extracted using trizol reagent (Invitrogen), subjected to 4% denaturing PAGE and visualized by autoradiography. A phosphoimager (Molecular Dynamics) was utilized for quantitative analysis of RNA stability over time.

In vitro translation

Extracts for *in vitro* translation were prepared as previously described (25) from 2 liters of HeLa S3 suspension cultures obtained from the Duke University Cell Culture Facility. *In vitro* translation reactions (40% HeLa extract, 3 ng/μl RNA, 20 mM creatine phosphate, 0.1 mg/ml creatine kinase, 0.1 mM spermidine, 100 mM amino acids, 16 mM HEPES, pH 7.4) were performed at 37°C. IRES mRNAs were translated in reactions containing 140 mM $K(OAc)_2$ and 2.5 mM $Mg(OAc)_2$; capped RNA reactions contained 40 mM $K(OAc)_2$ and 3 mM $Mg(OAc)_2$. Aliquots of 10 μl were removed at the indicated time points into an equal volume of stop solution (10 mM EDTA, 50 mg/ml RNase A) for measurements of RLuc activity. For RNA stability analysis, aliquots were removed into trizol (Invitrogen), extracted using the manufacturer's protocol and subjected to denaturing PAGE.

Sucrose gradients analysis

In vitro translation reactions were assembled as described above in the presence or absence of 0.5 mM cycloheximide. At the indicated time points, reactions were diluted in ice-cold gradient buffer (13), layered onto 5–20% sucrose gradients and centrifuged 37 000 r.p.m for 3 h and 45 min in a SW41 rotor. Absorbance spectra and fractions (0.52 ml) were obtained for each gradient using an ISCO density gradient fractionation system. Collected fractions were subjected to liquid scintillation counting (Beckman) or TCA precipitated for western blot analysis with α-RLuc antibody (Chemicon).

RESULTS

3′-Untranslated sequences influence HCV IRES-dependent translation *in vivo*

HCV translation was examined using monocistronic, subgenomic reporter RNAs that contain authentic *cis*-acting regulatory sequences derived from the infectious genotype 1a H77 strain (28). The parental reporter RNA, referred to as HCV16LUC, consists of the following structure: the entire HCV 5′-UTR plus the first 16 codons of the core coding region, the RLuc open reading frame (ORF) fused to five C-terminal codons from NS5B and the complete HCV 3′-UTR (Figure 1A). Core protein coding sequences immediately downstream of the 5′-UTR were included in HCV16LUC since they have been reported to stimulate HCV translation (29). The C-terminal NS5B codons were retained in order to preserve integrity of the predicted variable stem–loop 1 (VSL1) that is constituted by both coding and 3′-UTR sequences (Figure 1B).

   The capacity of HCV16LUC to direct translation in a cap-independent manner was tested by direct transfection of purified *in vitro* transcribed reporter RNA into Huh7 human hepatoma cells and analysis of RLuc accumulation at intermittent time points over the course of 10 h. A variant of HCV16LUC containing a 10 nt deletion of IRES domain IIIf (ΔIIIf; Figure 1A) that disrupts the conserved pseudoknot (30) was assayed in parallel as a negative control. HCV16LUC was efficiently translated compared to ΔIIIf which barely yielded detectable RLuc signal at 10 h post-transfection (Figure 1C), confirming the importance of higher order RNA structure in HCV IRES function and validating the reporter assay.

   Having established the functional competence of HCV16LUC in Huh7 cells, a potential role for the 3′-UTR in HCV gene expression was investigated. Huh7 cells were co-transfected with a capped mRNA encoding firefly luciferase for normalization of transfection efficiency and accumulated reporter proteins were quantified by enzymatic assay at 6 h post-transfection (see Materials and Methods). Initially, three RNAs based upon HCV16LUC with successive deletions from the 3′ end were examined (Figure 1B). Deletion of the X region resulted in a modest (∼50%) reduction in translation efficiency. In contrast, a more extensive deletion (3′Δpoly) in which both the poly(U/UC) tract and X region were removed consistently depressed RLuc accumulation >10-fold compared to the intact reporter RNA (Figure 2A). Deletion of the 43 nt variable region (3′ΔTD) further impaired reporter gene expression indicating that an intact 3′-UTR must be present to achieve maximal HCV translation. While modification of
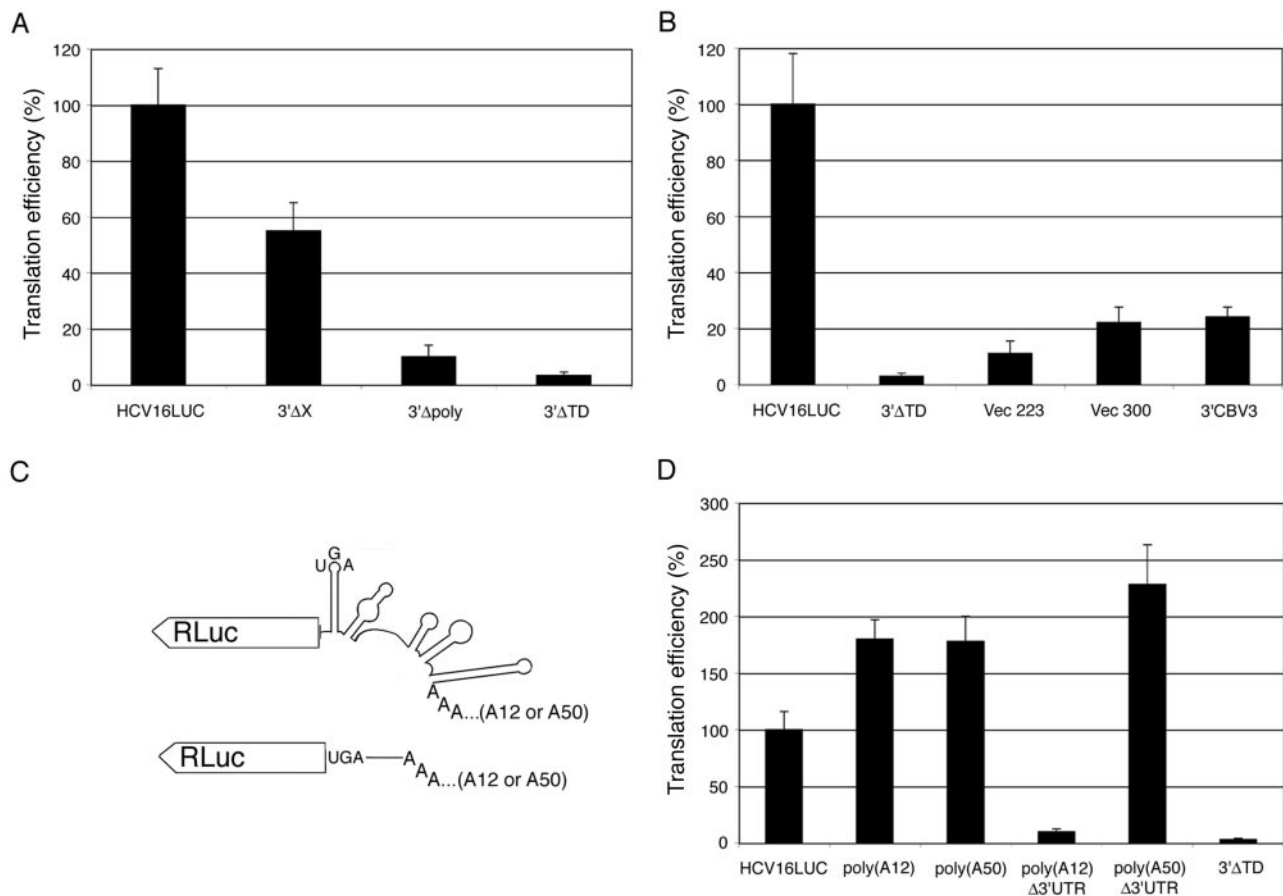
Figure 2. HCV IRES-dependent translation is stimulated by the cognate HCV 3′-UTR and artificial polyadenylation. Huh7 cells were co-transfected with the indicated reporter RNA and a second mRNA encoding firefly luciferase to control for variability of transfection efficiency. Six hours post-transfection, cell lysates were harvested for determination of luciferase activities. Translation efficiency of intact HCV16LUC was arbitrarily set at 100%. Error bars indicate standard deviation of three independently performed experiments. Effects of (**A**) progressive HCV 3′-UTR deletion, (**B**) substitution of the HCV 3′-UTR with non-specific sequences and (**D**) 3′ polyadenylation on RLuc expression are shown. A representation of the 3′ region of polyadenylated RNA constructs is illustrated in (**C**).

3′-UTR structures could conceivably result in an RNA stability phenotype, we were unable to detect substantial differences in decay rates of RNAs that exhibit widely divergent translation efficiencies (see below).

We next addressed the specificity of HCV translation enhancement by 3′-UTR sequences. For this purpose, the 3′-UTR of HCV16LUC was replaced with several unrelated sequences consisting of either (i) the coxsackievirus B3 (CBV3) 3′-UTR (3′CBV3), (ii) 223 nt of random vector sequence (Vec223; equal in length to the HCV 3′-UTR) or (iii) 300 nt of random vector sequence (Vec300). The CBV3 3′-UTR consists of three stable stem–loop domains (31) while the artificial vector-derived 3′-UTRs were predicted to lack extensive secondary structure features (data not shown). To exclude potential modulating effects due to poly(A), the CBV3 3′-UTR utilized in our constructs was non-polyadenylated. All unrelated 3′-UTRs improved translation directed by the HCV IRES relative to the 3′ΔTD construct (Figure 2B). However, translation directed by the native termini substantially outperformed each construct with a non-cognate 3′-UTR. The Vec300 construct was expressed at a higher level (∼2-fold) than Vec223, suggesting that length of the 3′-UTR alone may influence translation rate (32). However, translation of the CBV3 3′-UTR RNA exceeded that of Vec223 although the

former only comprises 100 nt (Figure 2B). This suggests a favorable effect on translation of stable secondary structures in the 3′-UTR. Taken together, these findings demonstrate that non-specific 3′-untranslated sequences enhance IRES-mediated translation compared to reporter RNA lacking a 3′-UTR, depending on their size and structural arrangement, but maximum translation efficiency requires the presence of the intact cognate 3′-UTR.

A 3′ poly(A) tail stimulates HCV translation rate

Polyadenylation has been reported to stimulate translation of IRES-containing picornavirus RNAs (25), possibly through promoting PABP-eIF4G interaction and resultant template circularization (33). In contrast to picornaviruses, the HCV genome neither terminates with poly(A) nor requires eIF4G for translation initiation. Consequently, poly(A) addition would not be expected to modulate function of the HCV IRES. This hypothesis was tested in Huh7 cells by examination of four HCV16LUC variants that possess a poly(A) tail of either 12 or 50 nts in length and either lack or include the native HCV 3′-UTR (Figure 2C). Assays performed with these RNAs revealed that polyadenylation of the HCV 3′-UTR with either 12 or 50 residues moderately elevated translation

compared to HCV16LUC (Figure 2D). In contrast, results obtained with polyadenylated RNAs lacking the HCV 3′-UTR varied dramatically with poly(A) tail length. Poly(-A12)Δ3′-UTR reporter RNA was translated at only 10% the level of HCV16LUC. However, an increase in poly(A) tail length from 12 to 50 nt resulted in a substantial increase (∼22 fold) in translation efficiency (Figure 2D). Thus, although HCV genomic RNA naturally lacks a poly(A) tail, artificial polyadenylation enhances translation rate *in vivo* and poly(A_{50}) can functionally substitute for the stimulatory role of the HCV 3′-UTR in translation.

3′-UTR manipulations do not affect RNA stability

Cellular mRNA turnover is intimately linked to translation and 3′ terminal structures have been shown to affect both processes [reviewed in (34)]. Consequently, experiments designed to assay translation rate as a function of 3′-UTR identity and polyadenylation state must take into account possible modulating effects of RNA stability. To address this possibility, we conducted experiments to assess the decay rate of select reporter RNAs that displayed dramatic differences in apparent translation activity.

Four reporter RNAs were selected for analysis of stability in Huh7 cells: HCV16LUC containing the intact HCV 3′-UTR; a variant with a complete 3′-UTR deletion (3′ΔTD); and RNAs that lack the HCV 3′-UTR but terminate with either poly(A_{12}) or poly(A_{50}). Huh7 cells were transfected with α-^{32}P-labeled reporter RNAs under conditions identical to those used in reporter experiments and soluble cytoplasmic RNA was isolated at multiple time points over the course of 10 h (see Materials and Methods). Radiolabeled RNAs were subsequently purified, visualized by denaturing gel electrophoresis (Figure 3A) and quantified using a phosphorimager (Figure 3B). Each RNA decayed at essentially equivalent rates, regardless of 3′-UTR status, with an apparent half-life of 6–8 h. These results suggest that stimulatory effects of the HCV 3′-UTR and poly(A_{50}) on IRES-driven translation are not mediated by increased reporter RNA stability.

HCV translation is influenced by 3′ terminal elements *in vitro*

While multiple reports have ascribed a positive role to the 3′-UTR in HCV translation, possible mechanism(s) responsible for this effect have not been uncovered. As an initial step towards this goal, we sought to recapitulate effects of 3′-UTR sequences on IRES-dependent translation in a tractable *in vitro* translation system. Rabbit reticulocyte lysate (RRL) is commonly used for *in vitro* translation studies. However, under standard conditions, RRL fails to mirror the synergistic activation of mRNA translation by the poly(A) tail and 5′ cap structure (19). We therefore utilized an *in vitro* translation extract derived from HeLa cells that reportedly exhibits poly(A) dependence for both capped and picornavirus IRES-harboring reporter RNAs (25). Reporter RNAs tested initially in Huh7 hepatoma cells were found to exhibit similar translation profiles in HeLa cells (data not shown). In addition, this cell-free system has been employed for recent mechanistic characterization of c-myc and BiP IRES function (35).

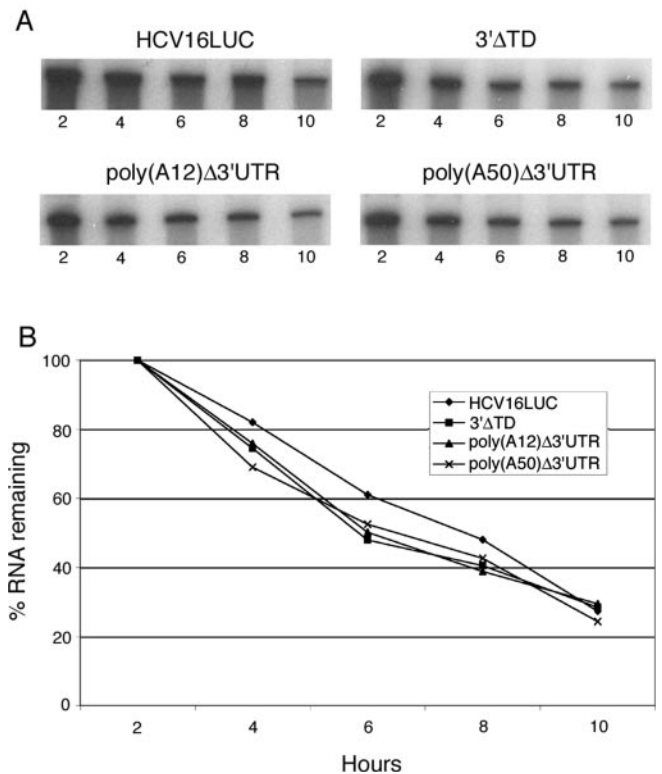To confirm responsiveness of HeLa cell extract to polyadenylation, capped RLuc mRNAs containing the 5′

Figure 3. Stability of HCV reporter RNAs is unaffected by 3′-UTR modification *in vivo*. (**A**) Radioactively labeled reporter RNAs were transfected into Huh7 cells. At the indicated time points (hours) after transfection, cells were lysed for isolation of soluble cytoplasmic RNA (see Materials and Methods). Extracted RNAs were separated by denaturing PAGE and visualized by autoradiography. (**B**) Intensities of radiolabeled RNA bands were quantitated using a phophorimager. RNA levels at 2 h after the start of transfection were set to 100%.

β-globin leader sequence were tested for translation activity as a function of poly(A) status. As expected, a capped mRNA lacking a poly(A) tail was an exceedingly poor translation template compared to an identical polyadenylated transcript (Figure 4A) with maximum reporter expression achieved after 10 min of incubation. The level of poly(A) responsiveness varied somewhat between extract preparations (between 20-fold and 50-fold stimulation of cap-dependent translation; data not shown). Decay rates of the radiolabeled capped mRNAs were compared next. Polyadenylation conferred a minor stabilizing effect (Figure 4B), in agreement with previous findings (25), indicating that differential expression of these mRNAs is largely the result of altered translation rates. Lastly, levels of *in vitro* 80S ribosomal complex accumulation on capped mRNAs were compared by sucrose density gradient fractionation (Figure 4C). Capped mRNA lacking a poly(A) tail displayed a reproducible, though modest, decrease (∼55%) in 80S complex formation compared to the cap-poly(A) reporter RNA. Thus, the cell-free translation system utilized recapitulates a role for 3′ polyadenylation in cap-dependent translation.

We subsequently examined HCV translation *in vitro*. Three reporter RNAs were selected for comparison with HCV16LUC based upon their variable performance in living cells: 3′ΔTD, poly(A12)Δ3′-UTR and poly(A50)Δ3′-UTR. These uncapped RNAs were incubated in cell extract and
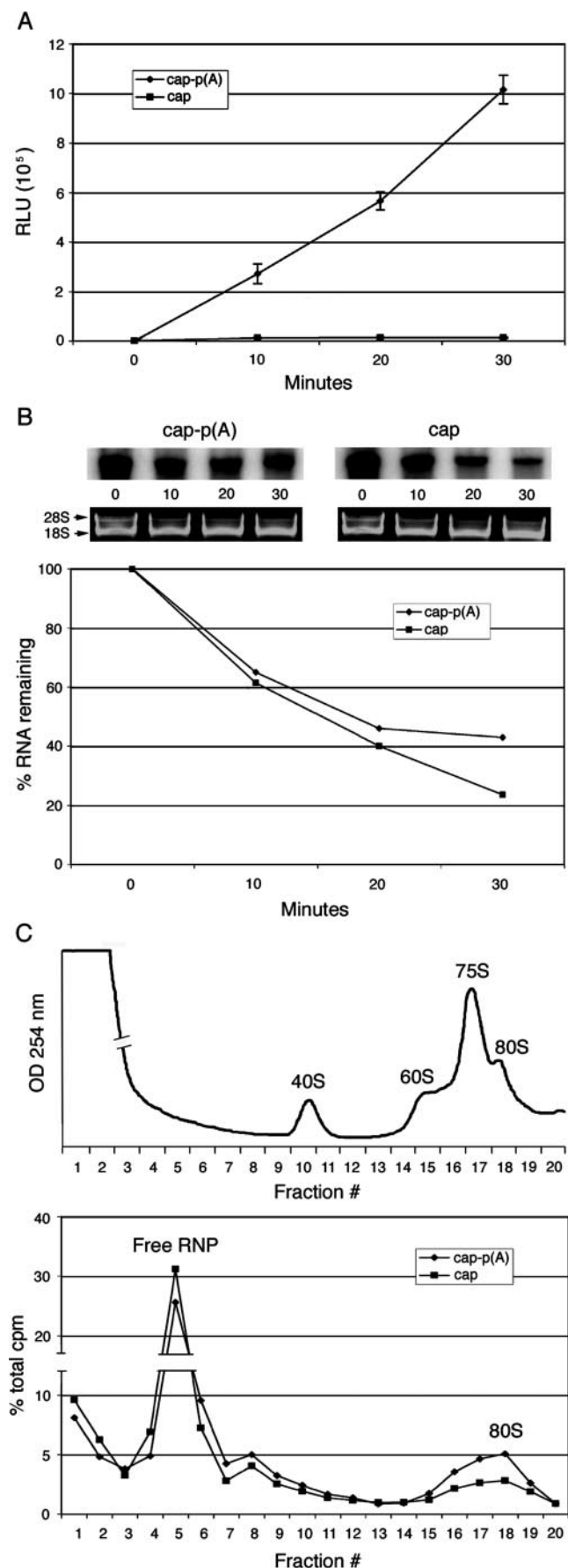
accumulation of RLuc was monitored at 10 min intervals over the course of 30 min (Figure 5A). The resulting pattern of translation activities resembled that observed *in vivo* (Figure 2D) although differences were relatively blunted. Significant divergence in translation efficiency of the reporter RNAs was apparent after 10 min of incubation. Reporter RNA lacking any 3′-UTR sequences translated weakly and addition of poly(A_{12}) increased performance by 7-fold. Both of these RNAs consistently failed to generate significant levels of reporter protein after 20 min of incubation. Importantly, addition of the HCV 3′-UTR or extension of the poly(A) tract to 50 residues substantially enhanced IRES-driven translation *in vitro* with linear synthesis of luciferase between 10 and 30 min time points, mirroring the poly(A) responsiveness observed for capped mRNAs.

As in cells, RNA stability was monitored *in vitro* over the time course of the experiment (Figure 5B and C) by tracking the decay of internally ^{32}P-labeled transcripts. Overall, differences in translation between reporter RNAs did not correlate with rates of decay. However, in contrast to experiments performed *in vivo*, RNA terminating in poly(A_{50}) displayed a moderate increase in half-life (∼2-fold) compared to other constructs which decayed at essentially identical rates. This stabilizing effect may be partially responsible for increased translation of poly(A50)Δ3′-UTR compared to HCV16LUC (Figure 5A). Notably, while poly(A) and the HCV 3′-UTR appear to be interchangeable in the promotion of effective IRES-mediated translation *in vitro*, the HCV 3′-UTR failed to confer a stabilizing effect.

First-round initiation at the HCV IRES is unaffected by 3′-untranslated sequences

Since the poly(A) tract and corresponding engagement of PABP have been previously implicated in multiple facets of initiation on capped mRNAs, we postulated that poly(A) or the HCV 3′-UTR might facilitate the formation of active 80S ribosomal complexes. Binary complex formation between the 40S ribosomal subunit and HCV IRES occurs with high affinity in the absence of either coding or 3′-UTR RNA (36). As a consequence, we specifically hypothesized that 3′ terminal elements may regulate formation of active 48S complexes and/or association of the 60S ribosomal subunit.

To address these possibilities, the accumulation of initiation intermediates on IRES-harboring RNAs was investigated

Figure 4. Polyadenyation stimulates cap-dependent translation at the level of initiation in a HeLa cell extract. (**A**) Extracts were programmed with 150 ng of either cap- or cap-poly(A) mRNA containing the β-globin leader sequence. Aliquots were removed at periodic intervals over the course of a 30 min incubation for measurements of luciferase activity. Error bars indicate standard deviation of reactions performed in triplicate. (**B**) Internally ^{32}P-labeled capped mRNAs were used to program *in vitro* translation reactions and decay was monitored over 30 min. Phophorimager analysis of band intensities is displayed. As a control for extraction and precipitation procedures, ribosomal RNAs (28S and 18S) from corresponding samples were visualized by native agarose gel electrophoresis. (**C**) Radiolabeled capped transcripts were assessed for their ability to incorporate into active 80S ribosomal complexes. Reactions were performed in the presence of 0.5 mM cycloheximide to prevent elongation. After 15 min of incubation at 37°C, reactions were diluted in chilled gradient buffer and loaded onto linear 5–20% sucrose gradients. Twenty fractions were collected from each gradient and analyzed by liquid scintillation counting. An absorbance profile indicating positions of ribosomal subunits and intact ribosomes is shown in the top panel.
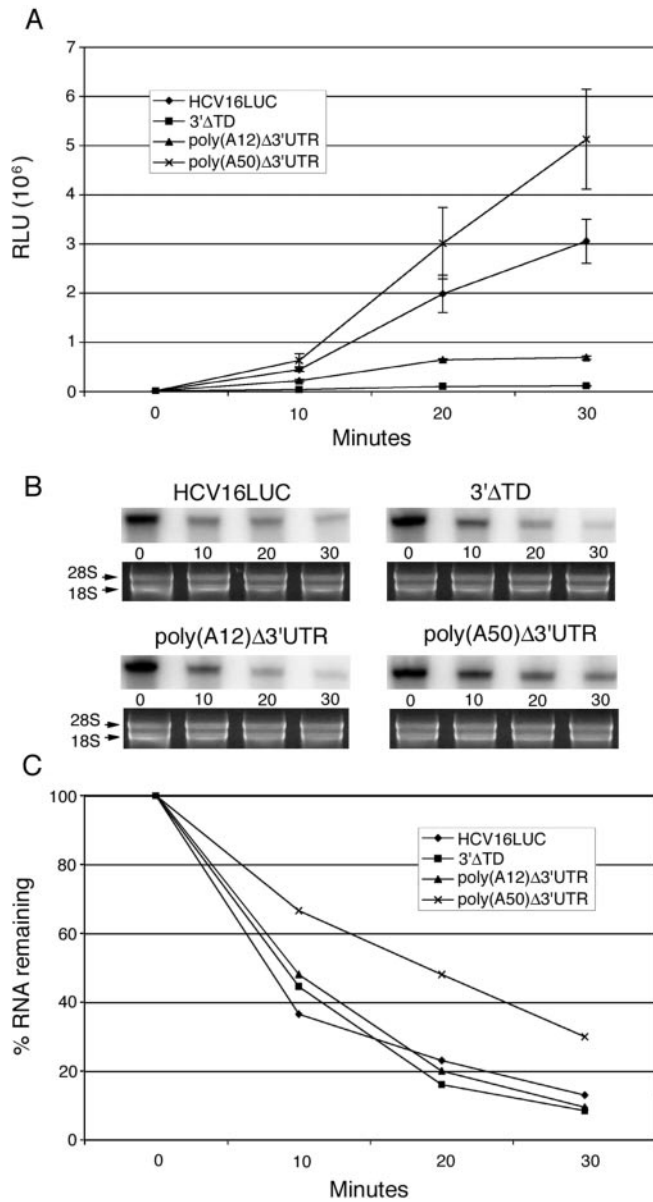
Figure 5. HCV IRES-driven translation is stimulated *in vitro* by poly(A) and the HCV 3′-UTR. *In vitro* translation reactions were programmed with the indicated uncapped HCV reporter RNAs for analysis of translation efficiency (**A**) and RNA stability (**B** and **C**) over the course of 30 min. Error bars indicate standard deviation. Ribosomal RNAs from corresponding samples were visualized by native agarose gel electrophoresis.

Figure 6. Ability of the HCV IRES to mediate the initiation phase of translation is unaffected by 3′-untranslated sequences. (**A**) The absorbance profile of a fractionated *in vitro* translation reaction is shown with positions of free ribosomal subunits and intact ribosomes indicated. The 75S peak represents mRNA-independent association of small and large ribosomal subunits (13). The lower panel shows the distribution of intact poly(A50)Δ3′-UTR reporter RNA at 2 min after start of the reaction by denaturing PAGE. (**B**) *In vitro* translation reactions were assembled in the presence of 0.5 mM cycloheximide and allowed to proceed for 2 min before addition of ice-cold gradient buffer to stop the reaction. Reactions were then subjected to sucrose density gradient centrifugation followed by fractionation. Individual fractions were analyzed for radioactivity levels by scintillation counting. (**C**) Same analysis as in (B) after 5 min of incubation at 37ºC.

using templates previously tested for *in vitro* translation efficiency (Figure 5). Radioactively labeled RNAs were incubated in translation extracts in the presence of cycloheximide to prevent commencement of elongation. Reactions were then subjected to density gradient centrifugation to separate ribosomal complexes and gradients were fractionated for analysis (see Materials and Methods). A representative absorbance profile indicating the positions of free subunits and ribosomes is shown in Figure 6A.

An initial time course experiment using HCV16LUC RNA indicated that accumulation of 80S complexes on this RNA occurred rapidly, reaching maximum at 5 min after
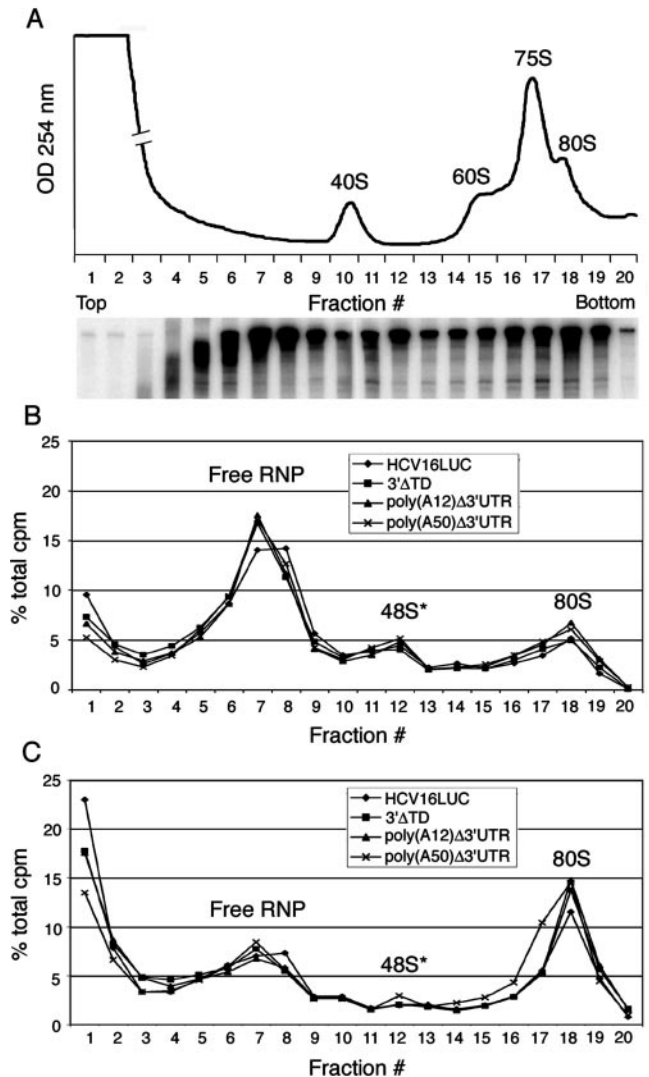
the start of incubation (Figure 6). Deletion of IRES domain IIIf (Figure 1A) completely blocked 80S complex formation (data not shown). Initiation performance of each RNA was examined after 2 (Figure 6B) and 5 min (Figure 6C) of incubation at 37°C. Three peaks of radioactive RNA were observed after 2 min, corresponding to intact RNA unassociated with ribosomal machinery, 48S* complexes and 80S ribosomes. The identity of the 48S* peak was confirmed using non-hydrolyzable GTP analog which prevents the 48S* to 80S transition (data not shown). At the later time point (Figure 6C), much of the 'free RNP' moved into either

80S peaks or accumulated at the top of the gradient as degraded fragments (Figure 6A, lower panel). No discernible peak representing binary IRES-40S complexes was observed, perhaps indicating rapid conversion of this intermediate to 48S* and 80S complexes. Importantly, only minor differences were apparent in the ability of different reporter RNAs to accumulate into 80S ribosomes. At the 5 min time point, the 80S peak for poly(A50)Δ3′-UTR was slightly larger in size than peaks for the remaining RNAs. However, this likely reflects the stabilizing effect of poly(A_{50}) on this RNA (Figure 5C) as indicated by lower radioactive counts present at the top of the gradient relative to other constructs (Figure 6C). The results of this analysis indicate that the HCV IRES is fully capable of executing the first round of translation initiation *in vitro* regardless of 3′-UTR identity. Consequently, the observed enhancement of HCV translation by polyadenylation or intact HCV 3′-UTR sequences must occur at a phase downstream of initiation.

Efficient translation termination is mediated by the HCV 3′-UTR or a poly(A) tail

Translating ribosomes that encounter an in frame stop codon associate with a complex of eukaryotic release factors, eRF1 and eRF3, that are responsible for directing hydrolysis of the peptidyl-transfer RNA (peptidyl-tRNA) bond by the 60S ribosomal subunit, resulting in release of the translated polypeptide from the ribosome. We sought to determine whether 3′ terminal elements that stimulate IRES-mediated translation *in vitro* directly enhanced efficiency of the termination reaction. For this purpose, the association of RLuc protein with actively translating ribosomes was investigated for each HCV reporter RNA variant to monitor the efficiency of polypeptide release. *In vitro* translation reactions were assembled to allow accumulation of RLuc and then subjected to density gradient centrifugation to separate free protein from ribosomal subunits and intact 80S ribosomes. Gradient fractions were then assayed for the presence of RLuc by immunoblot (see Materials and Methods for details). High molecular weight complexes containing RLuc protein were found to associate diffusely with fractions 7–9, containing 60S subunits and monosomes (Figure 7). The association of RLuc with heavy gradient fractions was disrupted in gradients containing EDTA which causes dissociation of ribosomal subunits (Figure 7B, lower panel).

As expected, reactions programmed with the efficiently translated HCV16LUC and poly(A50)Δ3′-UTR RNAs produced RLuc that existed primarily as free protein with lower levels of ribosome association (Figure 7B). In contrast, RLuc translated from reporter RNA with a 3′-UTR deletion (3′ΔTD) migrated to a substantially higher degree with monosomes, indicating inefficient release of RLuc protein from the template–ribosome complex. Interestingly, the gradient pattern of RLuc translated from the variant RNA containing a 12 residue poly(A) tail was similar to that of both active RNAs, with the majority of translation product free of ribosomal complexes. This indicates that a short poly(A) tail is sufficient to promote release of the translated polypeptide, but fails to stimulate overall translation to levels observed with a longer poly(A) tract. Taken together, these findings suggest that the non-polyadenylated HCV 3′-UTR and poly(A_{50})
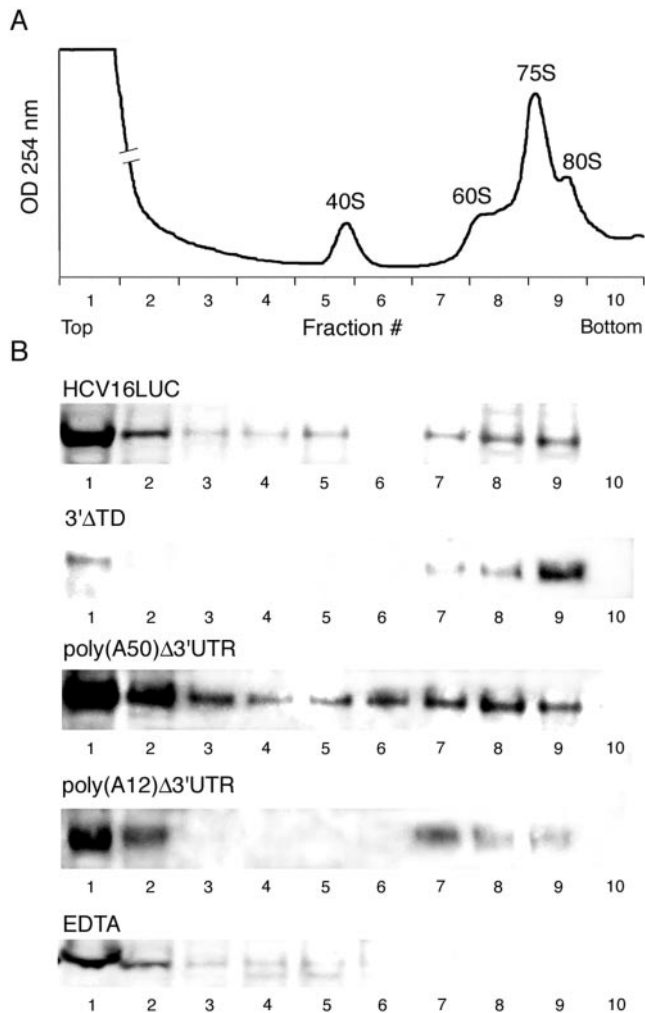

Figure 7. Analysis of translation termination *in vitro* by density gradient fractionation and immunoblot. (**A**) The absorbance profile of a fractionated *in vitro* translation reaction is shown with positions of free ribosomal subunits and intact ribosomes indicated. (**B**) *In vitro* translation reactions programmed with the indicated RNAs and incubated 30 min were fractionated by density gradient centrifugation. Individual fractions were TCA precipitated and separated by SDS–PAGE for western blot using α-RLuc antibody. As a control, an *in vitro* translation reaction programmed with HCV16LUC RNA was fractionated in the presence of 10 mM EDTA to disrupt association of ribosomal subunits, releasing RLuc to upper fractions of the gradient.

interchangeably enhance translation efficiency at and beyond the termination phase.

DISCUSSION

Regulation of translation rate is a critical aspect of gene expression control that depends on 5′ and 3′ terminal *cis*-acting elements within mRNAs. In conventional mRNAs, the 5′ cap and 3′ poly(A) tail provide the anchors for a ribonucleoprotein (RNP) bridge that activates translation (37). The potential for template closure also applies to translation of mRNAs with unorthodox terminal features (7,8,25,33). However, evidence for 5′-3′ interactions is lacking for the most unusual of translation templates: viral genomes of the flavivirus genera hepaci- and pestivirus that are devoid of both a cap and poly(A) tail.

We investigated the role of 3′ terminal structures in translation regulation with regard to the HCV 3′-UTR and its influence on gene expression at the cognate HCV IRES. Multiple previous studies have addressed a potential role for the HCV 3′UTR in modulating translation efficiency, but have yielded conflicting results. The sources of divergent experimental results are unclear. However, the structure of translation templates selected for analysis, methods used to express reporter constructs in cells and differential characteristics of distinct *in vitro* translation systems are potential confounding factors. The assay systems utilized here enabled examination of translation rate, initiation and termination efficiency, and lability of monocistronic subgenomic HCV reporter mRNAs with dissimilar 3′ terminal sequences. Extensive deletion or substitution of the native HCV 3′-UTR with non-specific sequences caused significant decline in IRES-mediated translation. Additionally, a poly(A) tract of 50 residues, sufficient in length to effectively recruit PABP (38), was able to fully replace the stimulatory effect of the HCV 3′-UTR on IRES-mediated translation.

Measurements of 80S complex formation on HCV IRES-driven RNAs *in vitro* revealed that modulation of IRES-dependent translation by either poly(A) or the HCV 3′-UTR occurs independently of the initiation phase. Indeed, even total 3′-UTR deletion from HCV16LUC, resulting in a 30-fold reduction in translation efficiency *in vitro*, had no discernible effect on the accumulation of 80S complexes. In Figure 5A significant differences in luciferase accumulation are evident after only 10 min of incubation. Given the rapid incorporation of HCV reporter RNAs into 80S complexes poised for elongation, we propose that multiple rounds of translation have occurred by this time point. Consequently, unlike initiation dependent on a 5′ cap structure, at least the first round of initiation mediated by the HCV IRES is unaffected by 3′-UTR identity.

The results presented here implicate the termination phase of translation to be critically influenced by 3′-UTR status. Two eukaryotic release factors, eRF1 and eRF3, facilitate the termination phase [reviewed in (39)]. Once elongating ribosomes encounter a stop codon, eRF1 associates with the ribosomal A-site and stimulates hydrolysis of the peptidyl-tRNA ester bond. The role of eRF3, a GTPase with affinity for eRF1, is less well understood, but it may promote rapid dissociation of eRF1 from the ribosome subsequent to release of the translated polypeptide based on studies of prokaryotic RF3 (40). Investigations in yeast suggest that, in the absence of a properly configured 3′-UTR, ribosomes terminate aberrantly and are slow to release from the mRNA template, resulting in translation repression (41,42). Moreover, aberrant termination can be reversed through tethering of PABP downstream of the stop codon, mimicking an authentic 3′-UTR. Poor translation of HCV reporter RNAs lacking either the authentic 3′-UTR or poly(A_{50}) may reflect inefficient release of ribosomes that terminate aberrantly. Indeed, the majority of translated RLuc protein remained bound to 80S ribosomes in the absence of 3′-untranslated sequences, suggesting the presence of stalled ribosomes at the mRNA 3′end.

A role for the 3′-UTR in accurate translation termination has previously been reported for the RNA genome of bovine viral diarrhea virus [BVDV; (43)], a flavivirus related to HCV. Extensive mutation of the variable region within the BVDV 3′-UTR caused an increase in ribosomal readthrough of the authentic stop codon and induced defective virus replication. Thus, while the BVDV 3′-UTR is distinct in both sequence and structure compared to that of HCV, both RNA segments appear to contain *cis*-acting signals that regulate viral translation. Interestingly, mutations resulting in a termination phenotype in BVDV also interfered with binding of the NFAR complex of cellular RNA-binding proteins to the variable region (44), suggesting a possible role for these factors in promoting accurate translation termination.

Besides modulation of the termination phase, stimulatory 3′-UTR elements could promote hypothetical recycling of ribosomal subunits in *cis* for subsequent rounds of initiation and elongation. The observation that poly(A_{12}) is sufficient for the polypeptide release step of termination, but fails to confer the stimulatory effect of poly(A_{50}), suggests that post-termination events may substantially influence overall translation rate. Template closure through juxtaposition of mRNA termini has been proposed to favor re-initiation of terminating ribosomes on the same RNA (37), implicating mechanistic differences between new initiation and successive initiation by ribosomes that have traversed the ORF (45). Although the possibility of ribosome recycling has not been physically demonstrated, our findings support such a hypothesis, implicating poly(A_{50}) or a functionally equivalent HCV 3′-UTR in post-termination events but not first-round initiation at the HCV IRES. Ribosome recycling may involve interaction between eRF3 and PABP (46) since disruption of this interaction has been reported to hinder cap-dependent translation without affecting accumulation of active 80S ribosome complexes (47). For the non-polyadenylated HCV 3′-UTR, an equivalent interaction potentially involved in control of viral gene expression has yet to be identified.

The stimulatory role of poly(A) in translation is well established for capped mRNAs and IRES-harboring picornaviral genomes (25,33). While it is clear that productive interaction between PABP and eIF4G improves the initiation phase of cap-dependent translation, the poly(A) tract may enable active translation via mechanisms that do not involve the initiation phase or conventional initiation factors. For example, recent investigation of c-myc and BiP IRES function has revealed an enhancing effect of the poly(A) tail that does not depend on intact eIF4G or PABP (35). In the context of the HCV IRES, poly(A) activates translation independently of the initiation phase, reflecting the unusual initiation mechanism utilized by the HCV genome that is independent of eIF4G and, possibly, PABP. Lastly, we observed relatively modest reduction in 80S formation on a capped-, non-polyadenylated mRNA despite a substantial reduction in overall translation, in agreement with previous experiments performed in PABP-depleted extract (4). Accordingly, we propose that a substantial contribution of the poly(A) tail to efficient cap-dependent translation occurs via mechanisms involving termination and post-termination events.

REFERENCES

1. Hershey,J.W.B. and Merrick,W.C. (2000) The pathway and mechanism of initiation of protein synthesis. In Sonenberg,N., Hershey,J.W.B. and Mathews,M.B. (eds), *Translational Control of Gene Expression*. Cold Spring Harbor Laboratory Press, Cold Spring Harbor, NY, pp. 33–88.

2. Mangus,D.A., Evans,M.C. and Jacobson,A. (2003) Poly(A)-binding proteins: multifunctional scaffolds for the post-transcriptional control of gene expression. *Genome Biol.*, **4**, 223.

3. Tarun,S.Z. and Sachs,A.B. (1996) Association of the yeast poly(A) tail binding protein with translation initiation factor eIF-4G. *EMBO J.*, **15**, 7168–7177.

4. Kahvejian,A., Svitkin,Y.V., Sukarieh,R., M'Boutchou,M.N. and Sonenberg,N. (2005) Mammalian poly(A)-binding protein is a eukaryotic translation initiation factor, which acts via multiple mechanisms. *Genes Dev.*, **19**, 104–113.

5. Searfoss,A., Dever,T.E. and Wickner,R. (2001) Linking the 3′ poly(A) tail to the subunit joining step of translation initiation: relations of Pab1p, eukaryotic translation initiation factor 5B (Fun12p), and Ski2p-Slh1p. *Mol. Cell Biol.*, **21**, 4900–4908.

6. Holden,K.L. and Harris,E. (2004) Enhancement of dengue virus translation: role of the 3′ untranslated region and the terminal 3′ stem–loop domain. *Virology*, **329**, 119–133.

7. Ling,J., Morley,S.J., Pain,V.M., Marzluff,W.F. and Gallie,D.R. (2002) The histone 3′-terminal stem–loop-binding protein enhances translation through a functional and physical interaction with eukaryotic initiation factor 4G (eIF4G) and eIF3. *Mol. Cell Biol.*, **22**, 7853–7867.

8. Piron,M., Vende,P., Cohen,J. and Poncet,D. (1998) Rotavirus RNA binding protein NSP3 interacts with eIF4GI and evicts the poly(A) binding protein from eIF4F. *EMBO J.*, **17**, 5811–5821.

9. Flamm,S.L. (2003) Chronic hepatitis C virus infection. *JAMA*, **289**, 2413–2417.

10. Tsukiyama-Kohara,K., Iizuka,N., Kohara,M. and Nomoto,A. (1992) Internal ribosome entry site within hepatitis C virus RNA. *J. Virol.*, **66**, 1476–1483.

11. Pestova,T.V., Shatsky,I.N., Fletcher,S.P., Jackson,R.J. and Hellen,C.U. (1998) A prokaryotic-like mode of cytoplasmic eukaryotic ribosome binding to the initiation codon during internal translation initiation of hepatitis C and classical swine fever virus RNAs. *Genes Dev.*, **12**, 67–83.

12. Ji,H., Fraser,C.S., Yu,Y., Leary,J. and Doudna,J.A. (2004) Coordinated assembly of human translation initiation complexes by the hepatitis C virus internal ribosome entry site RNA. *Proc. Natl Acad. Sci. USA*, **101**, 16990–16995.

13. Otto,G.A. and Puglisi,J.D. (2004) The pathway of HCV IRES-mediated translation initiation. *Cell*, **119**, 369–380.

14. Kolykhalov,A.A., Feinstone,S.M. and Rice,C.M. (1996) Identification of a highly conserved sequence element at the 3′ terminus of hepatitis C virus genome RNA. *J. Virol.*, **70**, 3363–3371.

15. Yanagi,M., St Claire,M., Emerson,S.U., Purcell,R.H. and Bukh,J. (1999) *In vivo* analysis of the 3′ untranslated region of the hepatitis C virus after *in vitro* mutagenesis of an infectious cDNA clone. *Proc. Natl Acad. Sci. USA*, **96**, 2291–2295.

16. Ito,T., Tahara,S.M. and Lai,M.M. (1998) The 3′-untranslated region of hepatitis C virus RNA enhances translation from an internal ribosomal entry site. *J. Virol.*, **72**, 8789–8796.

17. Ito,T. and Lai,M.M. (1999) An internal polypyrimidine-tract-binding protein-binding site in the hepatitis C virus RNA attenuates translation, which is relieved by the 3′-untranslated sequence. *Virology*, **254**, 288–296.

18. McCaffrey,A.P., Ohashi,K., Meuse,L., Shen,S., Lancaster,A.M., Lukavsky,P.J., Sarnow,P. and Kay,M.A. (2002) Determinants of hepatitis C translational initiation *in vitro*, in cultured cells and mice. *Mol. Ther.*, **5**, 676–684.

19. Michel,Y.M., Borman,A.M., Paulous,S. and Kean,K.M. (2001) Eukaryotic initiation factor 4G-poly(A) binding protein interaction is required for poly(A) tail-mediated stimulation of picornavirus internal ribosome entry segment-driven translation but not for X-mediated stimulation of hepatitis C virus translation. *Mol. Cell Biol.*, **21**, 4097–4109.

20. Fang,J.W. and Moyer,R.W. (2000) The effects of the conserved extreme 3′ end sequence of hepatitis C virus (HCV) RNA on the *in vitro* stabilization and translation of the HCV RNA genome. *J. Hepatol.*, **33**, 632–639.

21. Friebe,P. and Bartenschlager,R. (2002) Genetic analysis of sequences in the 3′ untranslated region of hepatitis C virus that are important for RNA replication. *J. Virol.*, **76**, 5326–5338.

22. Imbert,I., Dimitrova,M., Kien,F., Kieny,M.P. and Schuster,C. (2003) Hepatitis C virus IRES efficiency is unaffected by the genomic RNA 3′NTR even in the presence of viral structural or non-structural proteins. *J. Gen. Virol.*, **84**, 1549–1557.

23. Kong,L.K. and Sarnow,P. (2002) Cytoplasmic expression of mRNAs containing the internal ribosome entry site and 3′ noncoding region of hepatitis C virus: effects of the 3′ leader on mRNA translation and mRNA stability. *J. Virol.*, **76**, 12457–12462.

24. Murakami,K., Abe,M., Kageyama,T., Kamoshita,N. and Nomoto,A. (2001) Down-regulation of translation driven by hepatitis C virus internal ribosomal entry site by the 3′ untranslated region of RNA. *Arch. Virol.*, **146**, 729–741.

25. Bergamini,G., Preiss,T. and Hentze,M.W. (2000) Picornavirus IRESes and the poly(A) tail jointly promote cap-independent translation in a mammalian cell-free system. *RNA*, **6**, 1781–1790.

26. Ho,S.N., Hunt,H.D., Horton,R.M., Pullen,J.K. and Pease,L.R. (1989) Site directed mutagenesis by overlap extension using the polymerase chain reaction. *Gene*, **77**, 51–59.

27. Dobrikova,E., Flores,P., Bradrick,S. and Gromeier,M. (2003) Activity of a type 1 picornavirus internal ribosomal entry site is determined by sequences within the 3′ non-translated region. *Proc. Natl Acad. Sci. USA*, **100**, 15125–15130.

28. Yanagi,M., Purcell,R.H., Emerson,S.U. and Bukh,J. (1997) Transcripts from a single full-length cDNA clone of hepatitis C virus are infectious when directly transfected into the liver of a chimpanzee. *Proc. Natl Acad. Sci. USA*, **94**, 8738–8743.

29. Reynolds,J.E., Kaminski,A., Kettinen,H.J., Grace,K., Clarke,B.E., Carroll,A.R., Rowlands,D.J. and Jackson,R.J. (1995) Unique features of internal initiation of hepatitis C virus RNA translation. *EMBO J.*, **14**, 6010–6020.

30. Wang,C., Le,S.Y., Ali,N. and Siddiqui,A. (1995) An RNA pseudoknot is an essential structural element of the internal ribosome entry site located within the hepatitis C virus 5′ noncoding region. *RNA*, **1**, 526–537.

31. Pilipenko,E.V., Maslova,S.V., Sinyakov,A.N. and Agol,V.I. (1992) Towards identification of *cis*-acting elements involved in the replication of enterovirus and rhinovirus RNAs: a proposal for the existence of tRNA-like terminal structures. *Nucleic Acids Res.*, **20**, 1739–1745.

32. Tanguay,R.L. and Gallie,D.R. (1996) Translational efficiency is regulated by the length of the 3′ untranslated region. *Mol. Cell Biol.*, **16**, 146–156.

33. Svitkin,Y.V., Imataka,H., Khaleghpour,K., Kahvejian,A., Liebig,H.D. and Sonenberg,N. (2001) Poly(A)-binding protein interaction with eIF4G stimulates picornavirus IRES-dependent translation. *RNA*, **7**, 1743–1752.

34. Wilusz,C.J., Wormington,M. and Peltz,S.W. (2001) The cap-to-tail guide to mRNA turnover. *Nat. Rev. Mol. Cell Biol.*, **2**, 237–246.

35. Thoma,C., Bergamini,G., Galy,B., Hundsdoerfer,P. and Hentze,M.W. (2004) Enhancement of IRES-mediated translation of the c-myc and BiP mRNAs by the poly(A) tail is independent of intact eIF4G and PABP. *Mol. Cell*, **15**, 925–935.

36. Kieft,J.S., Zhou,K., Jubin,R. and Doudna,J.A. (2001) Mechanism of ribosome recruitment by hepatitis C IRES RNA. *RNA*, **7**, 194–206.

37. Jacobson,A. (1996) Poly(A) metabolism and translation: the closed loop model. In Sonenberg,N. (ed.), *Translational Control*. Cold Spring Harbor Laboratory Press, Cold Spring Harbor, NY, pp. 451–480.

38. Sachs,A.B., Davis,R.W. and Kornberg,R.D. (1987) A single domain of yeast poly(A)-binding protein is necessary and sufficient for RNA binding and cell viability. *Mol. Cell Biol.*, **7**, 3268–3278.

39. Kisselev,L., Ehrenberg,M. and Frolova,L. (2003) Termination of translation: interplay of mRNA, rRNAs and release factors? *EMBO J.*, **22**, 175–182.

40. Zavialov,A.V., Buckingham,R.H. and Ehrenberg,M. (2001) A posttermination ribosomal complex is the guanine nucleotide exchange factor for peptide release factor RF3. *Cell*, **107**, 115–124.

41. Amrani,N., Ganesan,R., Kervestin,S., Mangus,D.A., Ghosh,S. and Jacobson,A. (2004) A faux 3′-UTR promotes aberrant termination and triggers nonsense-mediated mRNA decay. *Nature*, **432**, 112–118.

42. Inada,T. and Aiba,H. (2005) Translation of aberrant mRNAs lacking a termination codon or with a shortened 3′-UTR is repressed after initiation in yeast. *EMBO J.*, **24**, 1584–1595.

43. Isken,O., Grassmann,C.W., Yu,H. and Behrens,S.E. (2004) Complex signals in the genomic 3′ nontranslated region of bovine viral diarrhea virus coordinate translation and replication of the viral RNA. *RNA*, **10**, 1637–1652.

44. Isken,O., Grassmann,C.W., Sarisky,R.T., Kann,M., Zhang,S., Grosse,F., Kao,P.N. and Behrens,S.E. (2003) Members of the NF90/NFAR protein group are involved in the life cycle of a positive-strand RNA virus. *EMBO J.*, **22**, 5655–5665.

45. Kuyumcu-Martinez,N.M., Van Eden,M.E., Younan,P. and Lloyd,R.E. (2004) Cleavage of poly(A)-binding protein by poliovirus 3C protease inhibits host cell translation: a novel mechanism for host translation shutoff. *Mol. Cell Biol.*, **24**, 1779–1790.

46. Hoshino,S., Imai,M., Kobayashi,T., Uchida,N. and Katada,T. (1999) The eukaryotic polypeptide chain releasing factor (eRF3/GSPT) carrying the translation termination signal to the 3′-Poly(A) tail of mRNA. Direct association of erf3/GSPT with polyadenylate-binding protein. *J. Biol. Chem.*, **274**, 16677–16680.

47. Uchida,N., Hoshino,S., Imataka,H., Sonenberg,N. and Katada,T. (2002) A novel role of the mammalian GSPT/eRF3 associating with poly(A)-binding protein in cap/poly(A)-dependent translation. *J. Biol. Chem.*, **277**, 50286–50292.